International Journal of Microwave and Wireless Technologies

cambridge.org/mrf

A dual-material strategy for enhancing the temperature robustness of microwave resonant cavity

Dongxu Fu, Xia Xiao and Linshuo Gu

Tianjin Key Laboratory of Imaging and Sensing Microelectronic Technology, School of Microelectronics, Tianjin University, Tianjin 300072, China

Research Paper

Cite this article: Fu D, Xiao X, Gu L (2023). A dual-material strategy for enhancing the temperature robustness of microwave resonant cavity. *International Journal of Microwave and Wireless Technologies* **15**, 1139–1146. https://doi.org/10.1017/S1759078722001404

Received: 8 August 2022
Revised: 13 November 2022
Accepted: 14 November 2022

Key words:
Microwave resonant cavity; resonant frequency; temperature robustness enhancement; dual-material strategy; temperature drift

Author for correspondence:
Xia Xiao, E-mail: xiaxiao@tju.edu.cn

Abstract

Resonant frequency varies significantly due to temperature changes for microwave resonant cavities. Hence, temperature robustness enhancement is of great importance. In this paper, a resonant cavity with enhanced temperature robustness is proposed by applying the dual-material strategy to the middle cavity. Compared to the single-material cavity, the dual-material cavity can demonstrate better temperature robustness with a decrease of 72.7% in the frequency shift over the temperature range of −20 to 80°C. Moreover, the $|S_{11}| < -10$ dB impedance bandwidth is 6.3% (3.39–3.61 GHz) and the gain is 20.4 dBi at 3.5 GHz for the manufactured dual-material cavity, which are much better than those of the manufactured single-material cavity. Finally, an experiment is conducted to measure the resonant frequencies with the sample solution tube of the dual-material cavity filled with nothing or 30 mg/dl $CuSO_4$ solution, the measured values are consistent with the simulated ones. The influence of temperature drift is significantly reduced, and the feasibility of the dual-material strategy is verified.

Introduction

Microwave resonant cavity is a type of sensor which is based on microwave measurement technology. It possesses the characteristics of highquality factor, low loss, and high stability. The primary working principle is the cavity perturbation technique, that is, the sample is tested assuming that the change in the internal state of the cavity before and after a small perturbation is almost the same [1–4]. When the resonant cavity meets the perturbation condition, the electromagnetic parameters of the substance can be measured based on the frequency variation of the resonant cavity, which helps to unify the characteristic parameters of the substance to be measured and the electromagnetic parameters of the microwave resonant cavity [5–7]. This helps to achieve accurate detection by using a resonant cavity. The specific working steps are as follows. An empty cavity is generated in the center of the closed conductor to form a microwave resonant cavity. The electromagnetic waves are reflected by the conductor wall of the cavity so that the electromagnetic energy oscillates in the process of mutual conversion. This helps to obtain the characteristic parameters of the resonant cavity. The electromagnetic waves in the position of the tested substance have the property of superposition, which can be used for analyzing some properties of the tested substance [8–10].

As a sensor, a resonant cavity is used to measure the permittivity of leaves in biology [11]. A rectangular resonant cavity is used to measure the salt and water content in the dried ham [12]. It is used in the medical industry such as medical cyclotrons [13], and to measure the humidity of the wet steam so as to improve the efficiency of steam turbine units in the mechanical industry [14].

The microwave resonant cavity is influenced by multiple physical fields, including electromagnetic field, temperature field, and stress field when it is working. The resonant cavity usually works in a wide temperature range. Due to the coefficient of thermal expansion of the materials, the resonant frequency changes as the cavity structure changes caused by the ambient temperature change, leading to a larger standing wave ratio, an increase in loss and phase offset, which is identified as temperature drift. If the variation in amplitude and phase caused by temperature drift exceeds a certain value, the transmission quality of the signal will decline, leading to large errors. Moreover, at high frequencies, microwave resonant cavity suffers from low gain, poor radiation efficiency and narrow bandwidth [15, 16]. Therefore, it is of great necessity to enhance the temperature performance of the resonant cavity [17].

At present, there are several methods to implement the temperature robustness enhancement of the resonant cavity. A resonant rod that can be automatically adjusted with temperature was used by Cogdell *et al.* to ensure that the capacitance between the resonant rod and the cavity remains unaltered [18]. The temperature performance enhancement with the help of a

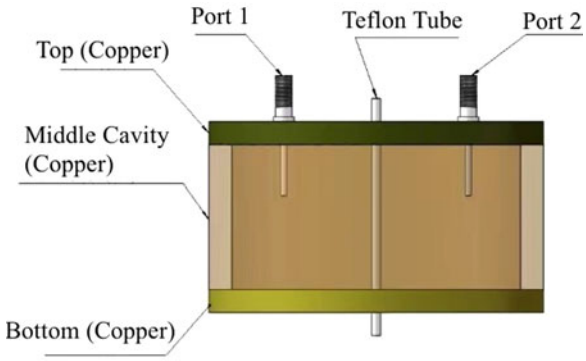

Fig. 1. Schematic configuration of the structure of the conventional cavity.

spring device made of Shape Memory Alloy (SMA) was achieved by Keats *et al.* [19]. The coefficient of thermal expansion of dielectric material and metal material was used by Sang-Kyu *et al.* to reduce the influence of temperature drift [20]. By monitoring two working modes of a specific resonant cavity, Cuenca *et al.* proposed a method to correct the influence of temperature on the system during the perturbation measurement of the resonant cavity [21]. A split degenerate TM_{m10} mode of the cylindrical cavity was innovatively designed by Barter *et al.* to enhance the temperature robustness [22].

In this paper, a resonant cavity with enhanced temperature performance and working mode of TM_{010}. Considering the compensation effect of the coefficient of thermal expansion of the materials, the approach of dual-material is presented. Coupling analysis of the electromagnetic field, steady-state thermal field and static structural field is set up to test the temperature performance of the single and dual-material cavities. Moreover, electromagnetic parameters of both cavities are compared such as the radiation pattern, $|S_{11}| < -10$ dB impedance bandwidth and gain. The simulated and measured results show that the dual-material cavity has better electromagnetic characteristics, and the dual-material strategy manages to enhance the temperature robustness.

This paper is organized as follows. Section 'Resonant cavity design' introduces the details of the resonant cavity design. Section 'Results and discussion' presents the simulation and experiment, together with corresponding results to demonstrate the performance of single and dual-material cavities. Finally, Section 'Conclusions' gives the conclusion to elaborate on the achieved results and discusses future work.

Table 1. Structure parameters of the conventional cavity

Structure parameters	Dimensions (mm)
Cavity radius	31.3
Cavity height	31.3
Inner radius of the tube	0.5
Outer radius of the tube	1.0
Length of SMA probe	11.0
Distance between SMA and tube	20.0

Resonant cavity design

Modal analysis of the conventional cavity

The cylindrical microwave resonant cavity is selected in this work because of its simple geometric structure and high inherent quality factor.

As demonstrated in Fig. 1, the conventional cavity is made of copper. Since the direction of the electric field near the axis of the cavity under TM_{010} mode is parallel to the axis and the electric field intensity is the maximum, the highest measurement sensitivity can be observed by placing the sample solution tube at this position. The probe coupling, through which energy exchanges between the resonant cavity and the outside space is realized by two SMA connectors positioned 20 mm away from the axis of the cavity. The height of the top and bottom is negligible since they just help to form a closed cavity. The resonant frequency of the empty cavity is approximately 3.5 GHz. The structure parameters of the conventional cavity are shown in Table 1.

In order to test the temperature robustness of the cavity, coupling analysis of the electromagnetic field, steady-state thermal field, and static structural field is set up in the finite element emulator and demonstrated in Fig. 2. The temperature range is set from −20 to 80°C, with the step of 10°C. Figure 3 shows the resonant frequency of the cavity with respect to the temperature. The resonant frequency of the conventional resonant cavity varies

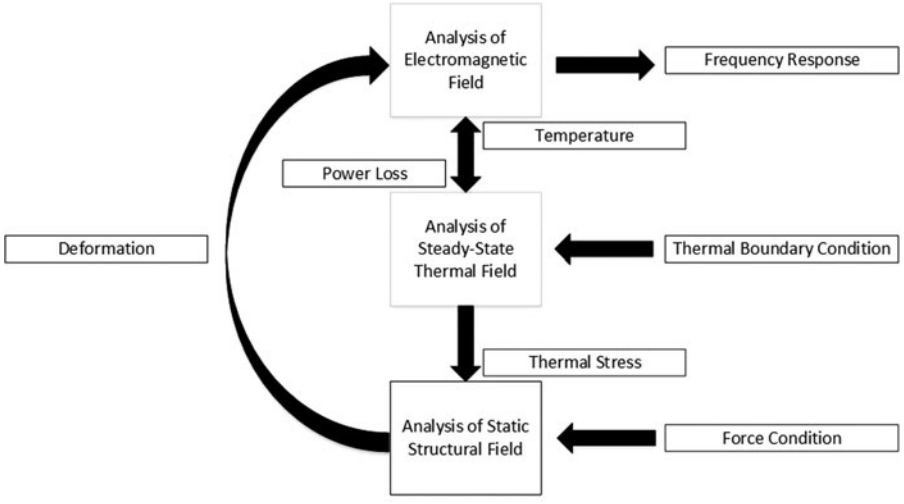

Fig. 2. Coupling analysis of electromagnetic field – steady-state thermal field – static structural field in finite element emulator.

https://doi.org/10.1017/S1759078722001404 Published online by Cambridge University Press

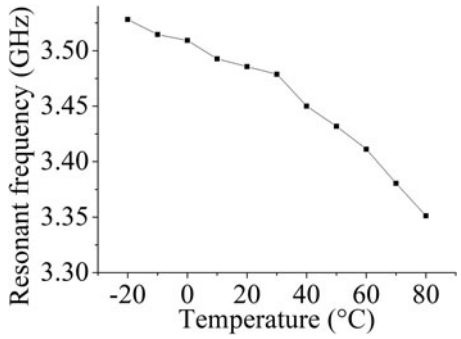

Fig. 3. Resonant frequency with respect to the temperature of the conventional cavity.

Table 2. Metal materials commonly used in the cavity and the coefficient of thermal expansion

Metals	Coefficients of thermal expansion (ppm/°C)
Aluminum	23.5
Invar	1.2
Brass	17.5
Titanium alloy	8.5
Stainless steel	13.1

significantly in a wide temperature operating range, which indicates that it has poor temperature robustness.

Dual-material strategy

According to the qualitative analysis results, the change of each dimension is determined by the coefficient of thermal expansion of the materials, nominal value, and temperature changes. The radius and height of the cavity increase with the increase in temperature, leading to a decrease in the resonant frequency [23]. In order to enhance the temperature robustness, the impact on the resonant frequency caused by the structure change of the cavity should be diminished or even eliminated. The temperature performance can thus be improved when the cavity radius and cavity height decrease as the temperature increases. Considering this, applying the dual-material strategy to the middle cavity is proposed. The key point is to optimize the ratio of the two materials.

Some common metals and coefficients of thermal expansion are listed in Table 2.

According to Table 2, brass and aluminum are the two preferred materials.

Parameter study

Figure 4 demonstrates the optimization results of cavity radius R, the distance between SMA and solution tube D_{SMA}, the best ratio of brass to aluminum L_1/L_2, and the height of the aluminum section $H_{Aluminum}$. According to the optimization results. $R = 29.8$ mm, $D_{SMA} = 17.0$ mm, $L_1/L_2 = 2.0$ and $H_{Aluminum} = 10.1$ mm are chosen for the cavity design.

Once the above optimization process is finished, the proposed dual-material cavity with good temperature robustness is derived, as demonstrated in Fig. 5. Compared to the conventional cavity, in the proposed cavity, the material of the top and bottom is replaced by brass, and the copper in the middle cavity is replaced by the combination of brass and aluminum. Table 3 shows the parameters of the proposed cavity.

Results and discussion

Validation by simulation

The analysis of the proposed cavity is conducted based on the research settings in Fig. 2. The corresponding cavity states at three temperatures of −20, 20 and 80°C are selected for comparison.

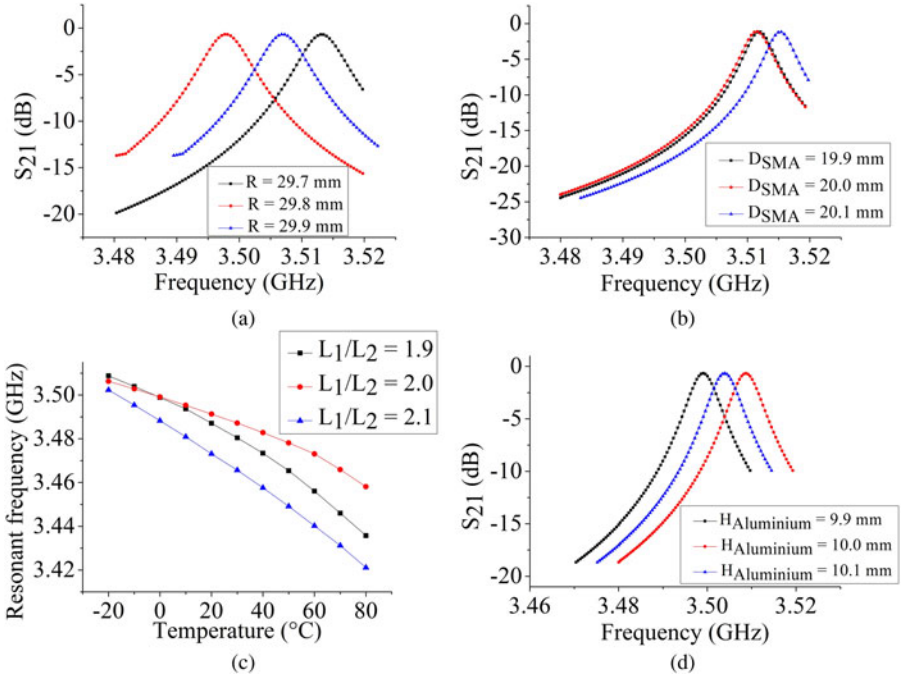

Fig. 4. Parameter optimization of (a) cavity radius, (b) distance between SMA and solution tube, (c) ratio of brass to aluminum, and (d) height of the aluminum section.

https://doi.org/10.1017/S1759078722001404 Published online by Cambridge University Press

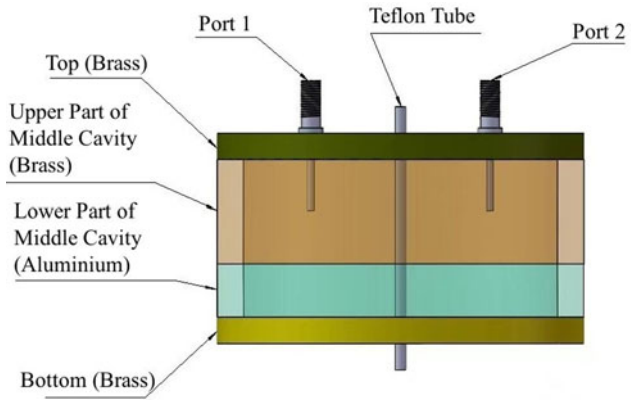

Fig. 5. Schematic configuration of the structure of the proposed cavity.

Table 3. Structure parameters of the proposed cavity

Structure parameters	Dimensions (mm)
Cavity radius	29.8
Cavity height	29.8
Inner radius of the tube	0.5
Outer radius of the tube	1.0
Length of SMA probe	14.6
Distance between SMA and tube	17.0
Height of the upper section	19.7
Height of the lower section	10.1

The results of the proposed cavity in the steady-state thermal field are demonstrated in Fig. 6. At temperatures of −20, 20 and 80°C, heat is uniform in all parts of the cavity after optimization and the three states are the same. This indicates a stable state in the wide temperature range.

Figure 7 demonstrates the results of the proposed cavity in the static structural field. The results suggest that the cavity has the same deformation state in a wide operating temperature range.

Figure 8 shows the measured and simulated results of the radiation pattern of two cavities. The results imply that there is better agreement between the measured and simulated results of the proposed cavity than that of the conventional cavity.

The variation of the resonant frequency of two cavities in a wide temperature range is tested. The temperature range is set from −20 to 80°C and the step is 10°C. Figure 9 shows the relationship between resonant frequency and temperature of the conventional and proposed cavities.

From −20 to 80°C, the resonant frequency of the conventional cavity changes from 3.5281 to 3.3512 GHz, with a percentage change of 5.014%, while the resonant frequency of the proposed cavity varies from 3.5163 to 3.4681 GHz, which is relatively stable with a percentage change of 1.371%. There is a decrease of 72.7% in the frequency shift. In addition, when the temperature exceeds 20°C, the resonant frequency of the conventional cavity decreases significantly. The results indicate that the temperature performance of the proposed cavity is significantly enhanced.

Validation by experiment

According to the parameters of Tables 1 and 3, the two cavities are produced and the manufactured dual-material cavity is demonstrated in Fig. 10.

After testing, the quality factor of the proposed cavity is 6425.52, which is much higher than that of the conventional cavity. According to Figs 11 and 12, the $|S_{11}| < -10$ dB impedance bandwidth of the manufactured proposed cavity is 6.3% (3.39–3.61 GHz) and gain is 20.4 dBi at 3.5 GHz, which is marginally different from the simulated results and much higher than those of the manufactured conventional cavity.

The test system is set up to test the enhancement effect of temperature performance of the manufactured proposed cavity.

As shown in Fig. 13, Vector Network Analyzer (VNA) is used to show the frequency curve and the thermostat is used to control the environmental temperature. The temperature range is set the same as the former test.

The measured resonant frequencies at different temperatures are measured and listed in Table 4 when the sample solution tube is empty, which are compared with the simulated results. The right side of the table shows the percentage errors relative to the simulated results. The measured values vary from 3.5238 to 3.4701 GHz. The average error with respect to the simulated results is 0.161%.

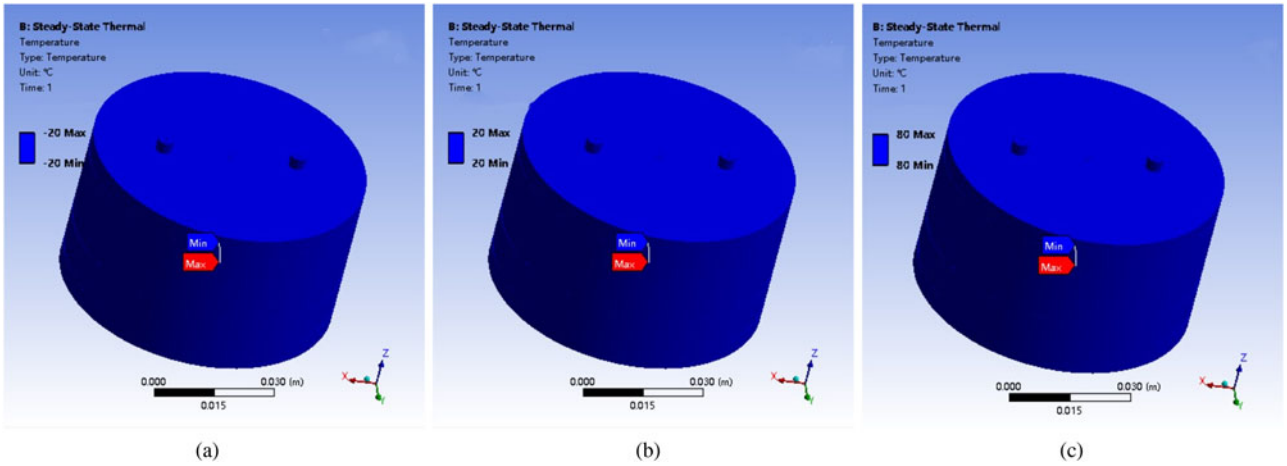

Fig. 6. Simulation results of the proposed cavity in the steady-state thermal field at (a) −20°C, (b) 20°C, and (c) 80°C.

https://doi.org/10.1017/S1759078722001404 Published online by Cambridge University Press

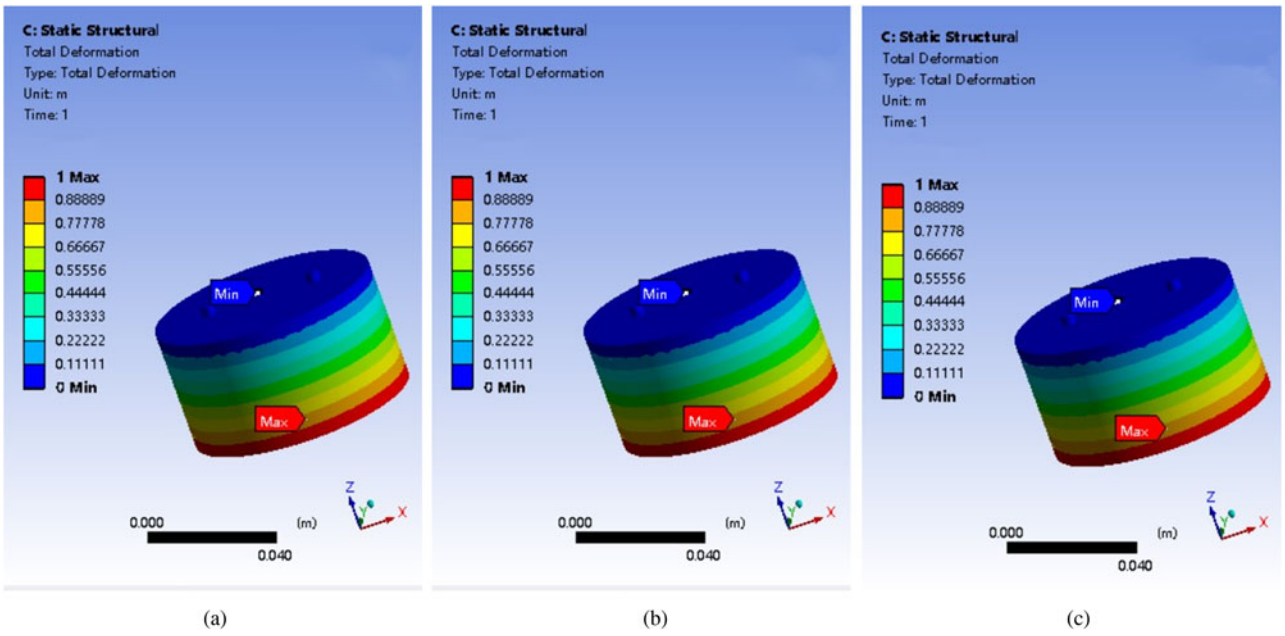

Fig. 7. Simulation results of the proposed cavity in the static structural field at (a) −20°C, (b) 20°C, and (c) 80°C.

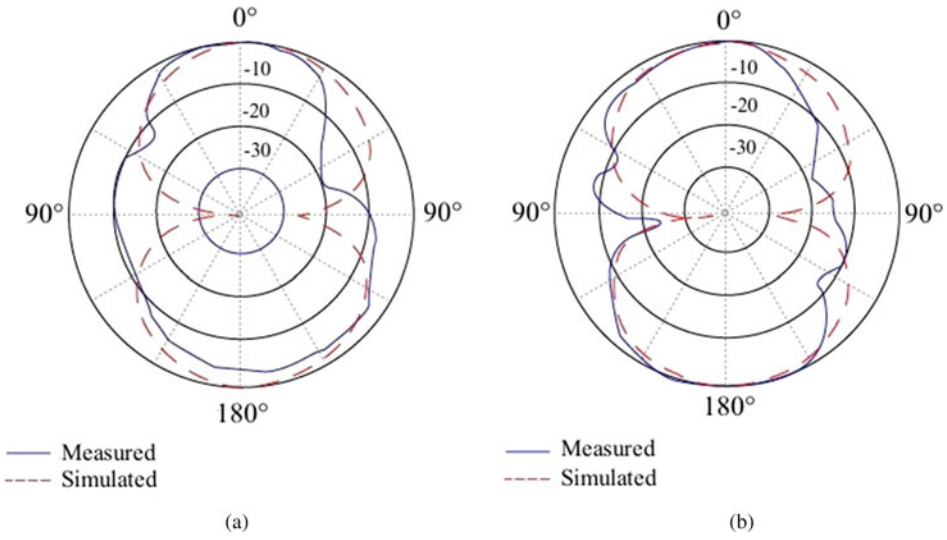

Fig. 8. Measured and simulated radiation pattern results on X–Z plane of (a) conventional cavity, and (b) proposed cavity.

For further testing of the cavity's temperature performance, 30 mg/dl $CuSO_4$ solution is used. The results are listed in Table 5. Under the same temperature condition, there is an average error between the measured values and the simulated values, which is 0.154%. The results show that the difference between the simulated and measured values is small, which indicates the feasibility of the dual-material strategy.

Conclusions

In this paper, a microwave resonant cavity with enhanced temperature robustness is proposed, in which the dual-material approach is applied to enhance the temperature robustness. Coupling analysis of the electromagnetic field, steady-state thermal field, and static structural field is set up to test the temperature robustness. The simulated results indicate that the heating condition and cavity deformation of the dual-material cavity at different temperatures remain the same in a wide temperature range, and the resonant frequency is relatively stable with the resonant frequency percentage change of 1.371%, which is better than that of the single-material cavity. Based on the experimental results, the high-quality factor, compatibility of the radiation pattern and gain, together with the $|S_{11}| < -10$ dB impedance bandwidth of 6.3% are achieved for the dual-material cavity, which are obviously better than those of the single-material cavity. The dual-material cavity is fabricated to verify the design method, and the measured results agree well with the simulated ones demonstrating high temperature robustness. The results indicate that the dual-material cavity has better electromagnetic characteristics, and the proposed strategy is feasible. Moreover,

https://doi.org/10.1017/S1759078722001404 Published online by Cambridge University Press

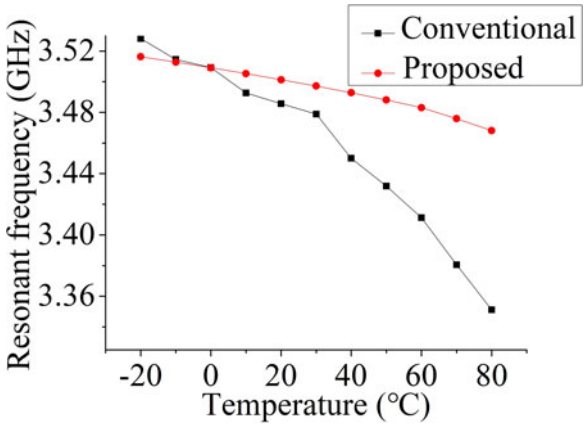

Fig. 9. Resonant frequency with respect to the temperature of the conventional cavity and proposed cavity.

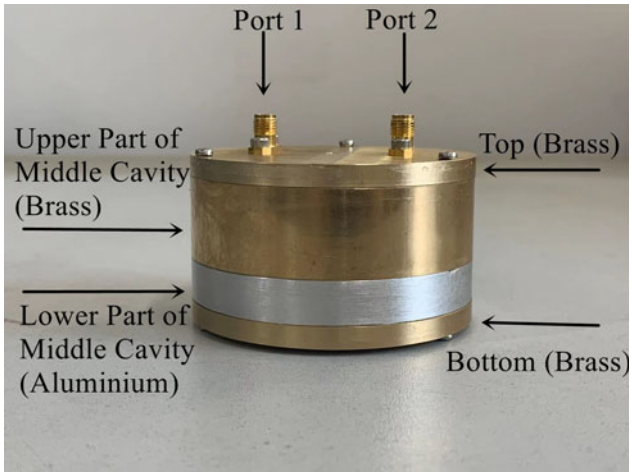

Fig. 10. The manufactured dual-material cavity.

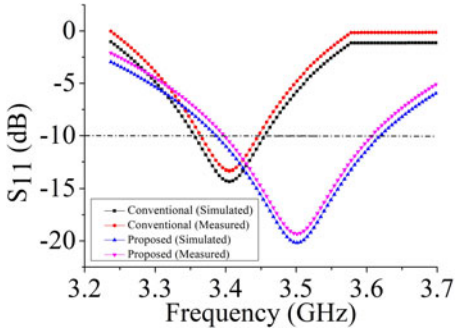

Fig. 11. S_{11} of the conventional cavity and proposed cavity.

the high-quality factor, gain values and temperature robustness make the resonant cavity suitable for high-accuracy solution concentration measurement.

Based on this work, more research can be conducted on temperature compensation algorithms in the future to further enhance the temperature robustness of the cavity. The dual-material strategy can be applied to other sensors to verify its universality. Apart from the solution concentration measurement, gas or gas-liquid mixture concentration measurement can be carried out by using the dual-material cavity.

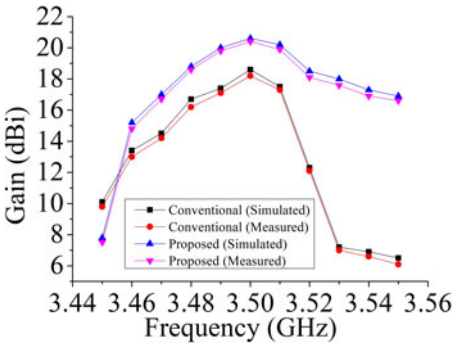

Fig. 12. Gain of the conventional cavity and proposed cavity.

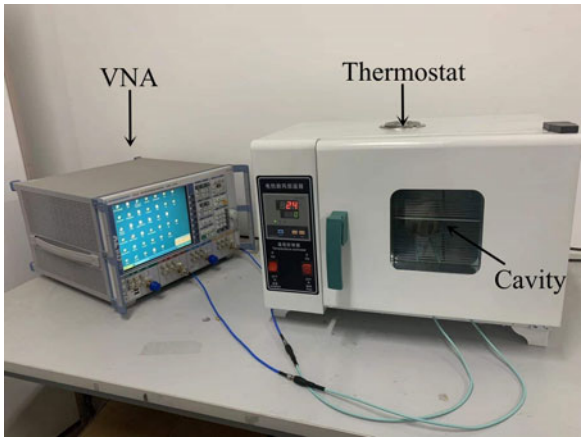

Fig. 13. The system for the temperature stability test.

Table 4. Comparison of the simulated and measured results of the proposed cavity

	Resonant frequencies (GHz)		
Temperatures (°C)	Proposed (simulated)	Proposed (measured)	Percentage errors (%)
−20	3.5163	3.5238	0.213292
−10	3.5128	3.5201	0.207811
0	3.5091	3.5163	0.205181
10	3.5053	3.5123	0.199698
20	3.5013	3.5080	0.191357
30	3.4972	3.5035	0.180144
40	3.4928	3.4985	0.163193
50	3.4881	3.4932	0.146211
60	3.4831	3.4863	0.091872
70	3.4759	3.4797	0.109324
80	3.4681	3.4701	0.057668

The sample solution tube is empty.

Data. Research data are not shared.

Author contributions. Xia Xiao and Dongxu Fu derived the theory. Linshuo Gu and Dongxu Fu performed the simulations and experiments. All authors

https://doi.org/10.1017/S1759078722001404 Published online by Cambridge University Press

Table 5. Comparison of the simulated and measured results of the proposed cavity

Temperatures (°C)	Resonant frequencies (GHz)		
	Proposed (simulated)	Proposed (measured)	Percentage errors (%)
−20	3.5333	3.5405	0.203776
−10	3.5299	3.5367	0.192640
0	3.5262	3.5331	0.201361
10	3.5224	3.5292	0.193050
20	3.5181	3.5246	0.184759
30	3.5142	3.5203	0.173581
40	3.5097	3.5154	0.162407
50	3.5053	3.5102	0.134083
60	3.5006	3.5037	0.085714
70	3.4932	3.4966	0.103063
80	3.4851	3.4869	0.054519

The sample solution tube is filled with 30 mg/dl $CuSO_4$ solution.

contributed equally to analyzing data and reaching conclusions, and in writing the paper.

Financial support. This research received no specific grant from any funding agency, commercial or not-for-profit sectors.

Conflict of interest. The authors report no conflict of interest.

References

1. **Qiao L, Xia X, Hao F and Liang W** (2018) Glucose solution concentration detection using TE_{011} microwave resonant cavity. *Journal of Electromagnetic Waves and Applications* **32**, 1824–1833.
2. **Peter R and Fischerauer G** (2018) De-embedding method for strongly coupled cavities. *IEEE Transactions on Microwave Theory and Techniques* **66**, 2025–2033.
3. **Ivanchenko I, Khruslov M, Popenko N, Plakhtii V and Tkach V** (2020) Modified cavity perturbation method for high-precision measurements of complex permittivity throughout the X-band. *Microwave and Optical Technology Letters* **62**, 3180–3185.
4. **Marchal F, Yousfi M and Merbahi N** (2016) Quantitative determination of density of ground state atomic oxygen from both TALIF and emission spectroscopy in hot air plasma generated by microwave resonant cavity. *Plasma Science and Technology* **18**, 259.
5. **Kim CK, Minz L and Park SO** (2007) Improved measurement method of material properties using continuous cavity perturbation without relocation. *IEEE Transactions on Instrumentation and Measurement* **69**, 5702–5716.
6. **Miura T and Tahara K** (2005) Frequency-dependent permeability evaluation by harmonic resonance cavity perturbation method. *IEEE Transactions on Microwave Theory and Techniques* **68**, 1773–1782.
7. **Tian Q and Wang C** (2017) Quantitative detection of glucose level based on radiofrequency patch biosensor combined with volume-fixed structures. *Biosensors and Bioelectronics* **98**, 357–363.
8. **Tsankova G, Richter M and Madigan A** (2016) Characterisation of a microwave re-entrant cavity resonator for phase-equilibrium measurements and new dew-point data for a (0.25 argon + 0.75 carbon dioxide) mixture. *The Journal of Chemical Thermodynamics* **101**, 395–404.
9. **Berry GG, Sagi O and Markus BG** (2018) A highly accurate measurement of resonator Q-factor and resonance frequency. *Review of Entific Instruments* **89**, 2459–2487.
10. **Chao HW and Chang TH** (2018) Wide-range permittivity measurement with a parametric-dependent cavity. *IEEE Transactions on Microwave Theory and Techniques* **66**, 4641–4648.
11. **Chengyu L** (2007) Microwave cavity perturbation method to measure the permittivity of plant leaves. *Journal of Changchun Normal University (Natural Science Edition)* **26**, 44–46.
12. **Bjarnadottir SG, Lunde K and Alvseike O** (2015) Assessing quality parameters in dry-cured ham using microwave spectroscopy. *Meat Science* **108**, 109–114.
13. **Junwang G** (2006) Analysis of RF cavity for a small medical cyclotron with low energy by FEM. *Journal of Huazhong University of Science and Technology, Nature Science* **34**, 65–67.
14. **Jiangbo Q** (2012) Theoretical analysis of cavity perturbation techniques for measuring wet steam tow-phase flow. *Proceedings of the Chinese Society of Electrical Engineering* **32**, 79–85.
15. **Bilal HM, Angel PC, Cleofas SG, Ruiz FG and Padilla P** (2021) SIW cavity-backed antenna array based on double slots for mmWave communications. *Applied Science-Basel* **11**, 4824.
16. **Chemweno EK, Kumar P and Afullo Thomas JO** (2022) Substrate integrated waveguide-dielectric resonator antenna for future wireless communication. *SAIEE Africa Research Journal* **113**, 119–128.
17. **Chorom J, Jin-Kwan P, Hee-Jo L, Gi-Ho Y and Jong-Gwan Y** (2018) Temperature-corrected fluidic glucose sensor based on microwave resonator. *Sensors (Basel, Switzerland)* **18**, 3850.
18. **Cogdell JR, Deam AP and Straition AW** (1960) Temperature compensation of coaxial cavities. *IRE Transactions on Microwave Theory & Techniques* **8**, 151–155.
19. **Keats BF, Gorbet RB and Mansour RR** (2003) Designed and testing of SMA temperature-compensated cavity resonators. *IEEE Transactions on Microwave Theory & Techniques* **51**, 2284–2289.
20. **Sang-Kyu L, Han-Young L, Jun-Chul K and Chul A** (1999) The design of a temperature-stable stepped-impedance resonator using composite ceramic materials. *IEEE Microwave and Guided Wave Letters* **9**, 143–144.
21. **Cuenca JA, Slocombe DR and Porch A** (2017) Temperature correction for cylindrical cavity perturbation measurements. *IEEE Transactions on Microwave Theory and Techniques* **65**, 2153–2161.
22. **Barter M, Partridge S, Slocombe DR and Porch A** (2019) Temperature correction using degenerate modes for cylindrical cavity perturbation measurements. *IEEE Transactions on Microwave Theory and Techniques* **67**, 800–805.
23. **Chi W and Kawthar AZ** (1999) Temperature compensation of combline resonators and filters. *1999 IEEE MTT-S International Microwave Symposium Digest*. (Cat. No.99CH36282) Anaheim, CA, USA, pp. 1041–1044. doi: 10.1109/MWSYM.1999.779566.

Dongxu Fu obtained his B.S. in electronic information science and technology from the University of Shanghai for Science and Technology, Shanghai, China, in 2020. Currently, he is a master student of integrated circuit engineering at Tianjin University. His research interests include the temperature robustness enhancement of microwave resonant cavity, electromagnetic properties of microwave resonant cavity, solution concentration measurement methods and systems based on microwave perturbation technology.

Xia Xiao obtained her B.S. in physics and M.S. in condensed physics from Tianjin Normal University, Tianjin, China, in 1993 and 1996, respectively, and the Ph.D. in electronic and information technology from the Technical University of Chemnitz, Germany, in 2002. From 2007 till now, she is a professor in Tianjin University. Her research interests include the electromagnetic characteristics of microwave resonant cavity, target detection by UWB microwave imaging, non-invasive blood glucose by microwave detection, and non-destructive characterization of film properties by surface acoustic waves.

https://doi.org/10.1017/S1759078722001404 Published online by Cambridge University Press

Linshuo Gu obtained his B.S. in electronic science and technology from Hebei University of Technology, Tianjin, China, in 2017. Currently, he is a master student of integrated circuit engineering at Tianjin University. His research interests include the solution concentration measurement methods and systems based on microwave perturbation technology.

https://doi.org/10.1017/S1759078722001404 Published online by Cambridge University Press